

## Advances in $^{211}\text{At}$ production at Texas A&M University

S.J. Yennello<sup>1,2,\*</sup>, L.A. McIntosh<sup>1</sup>, J.D. Burns<sup>3</sup>, E.E. Tereshatov<sup>1</sup>, G. Tabacaru<sup>1</sup>, L. McCann<sup>1,2</sup>, S. Schultz<sup>1,2</sup>, K. Lofton<sup>1,2</sup>, A. Abbott<sup>1</sup>, G. Avila<sup>1</sup>, M. Berko<sup>1,4</sup>, E. Engelthaler<sup>1,5</sup>, K. Hagel<sup>1</sup>, A. Hannaman<sup>1</sup>, B. Harvey<sup>1</sup>, A. Hood<sup>1</sup>, M. McCarthy<sup>1</sup>, A.B. McIntosh<sup>1</sup>, M. Sorensen<sup>1</sup>, Z Tobin<sup>1</sup>, and A. Vonder Haar<sup>1</sup>

<sup>1</sup>Cyclotron Institute, Texas A&M University, College Station, TX, USA

<sup>2</sup>Department of Chemistry, Texas A&M University, College Station, TX, USA

<sup>3</sup>Nuclear Engineering and Science Center, Texas A&M University, College Station, TX, USA

<sup>4</sup>New Jersey Institute of Technology, Newark, NJ, USA

<sup>5</sup>University of Dallas, Dallas, TX, USA

**Abstract.** Alpha emitting radionuclides with medically relevant half-lives are interesting for treatment of tumors and other diseases because they deposit large amounts of energy close to the location of the radioisotope. Researchers at the Cyclotron Institute at Texas A&M University are developing a program to produce  $^{211}\text{At}$ , an alpha emitter with a medically relevant half-life. The properties of  $^{211}\text{At}$  make it a great candidate for targeted alpha therapy for cancer due to its short half-life (7.2 h). Astatine-211 has now been produced multiple times and reliability of this process is being improved.

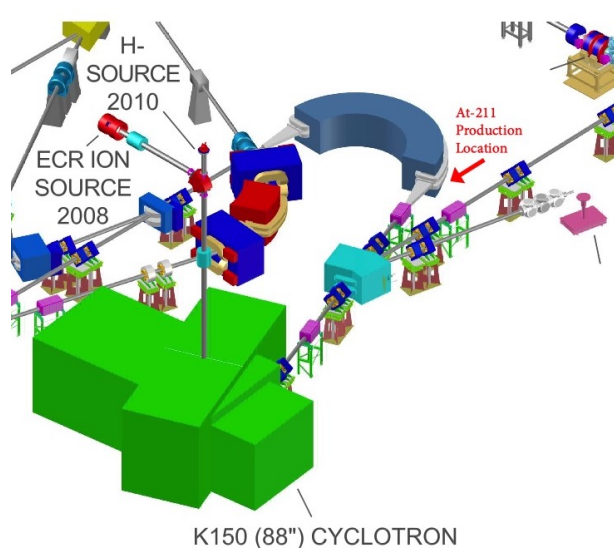


**Figure 1.** Isotope production line from K150 cyclotron.

### 1 Introduction

While radioisotopes have long been used to treat cancer, the ability to specifically target cancerous cells has only been available in special cases. With the advent of targeting agents such as monoclonal antibodies, the ability to use radioisotopes which deposit a large amount of energy and do not move far from the targeting agent has become an area of considerable interest. Targeted alpha therapy is taking advantage of these advances to use alpha emit-

ters with biologically relevant half lives. Astatine (At) has emerged as an element of interest for these purposes. There are no known stable isotopes of astatine. The small amounts of At present in the Earth's crust are due to the decay of other elements. Natural presence of astatine is very fleeting as no astatine isotope has a half-life greater than 8 hours.

Targeted alpha therapy drugs [1–11] have gained a large amount of interest following the success of Xofigo®, [12] based on the  $\alpha$  emitting  $^{223}\text{RaCl}_2$ , in treating metastatic castration-resistant prostate cancer. Astatine-211 shows promise for cancer treatments when connected to a targeting agent, especially for non-localized cancers [7]. The major impediment to its use in clinical trials remains the availability of production and reliable separation chemistry [8, 13]. However, because of its short half-life, a rapid system with high yield is necessary for recovering the  $^{211}\text{At}$ .

At the Cyclotron Institute (CI) at Texas A&M University we have developed the ability to produce  $^{211}\text{At}$  by bombardment of a natural Bi target with an alpha beam from the K150 cyclotron and developed a purification system based on a newly discovered chemical interaction of At with a class of chemicals known as ketones.

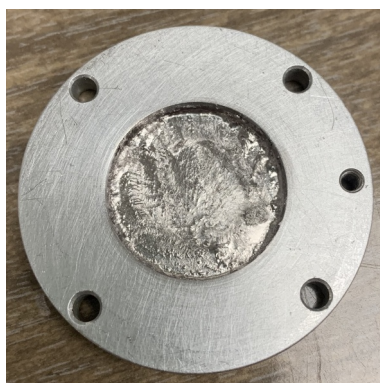
### 2 At-211 production

Astatine-211 is produced via a nuclear reaction resulting from a metal plate of bismuth (Bi) being bombarded by  $\alpha$ -particles [13–17] accelerated by the Texas A&M K150 cyclotron shown in Figure 1. The  $^{211}\text{At}$  is trapped in the Bi target and needs to be extracted through a chemical process. Generally completely dissolving the target followed

\*e-mail: yennello@tamu.edu

**Table 1.** At-211 production. The plus signs denote irradiations done using the  $2^+$  charge state of the alpha beam, activities were calculated using a different method for the asterisks (\*).

Irradiations	Max Beam ( $\mu\text{A}$ )	Ave Beam ( $\mu\text{A}$ )	Irr time (h)	Activity at EoB (mCi)
December 2019 <sup>+</sup>	4.4	2.7	8	$24 \pm 2$
March 2020 <sup>+</sup>	3.5	3.2	9	$41 \pm 3$
June 2020	4.5	2.1 (Unstable)	9.4	$8.0 \pm 1.3$
August 2020	2.6	2.4	9.6	$21 \pm 2$
September 2020	7.4	5.1	7.3	$22 \pm 2^*$
October 2020	5	4.0	7.9	$12 \pm 1$
November 2020	7.2	4.2	9.7	$24 \pm 2$
December 2020	6.8	4.8	13.6	$47 \pm 5^*$
April 2021	8.2	5.61	15.6	$17 \pm 2$
May 2021	5	3.36	15.5	$11 \pm 1$
June 2021a	8.4	6.5	15.3	$24 \pm 3$
June 2021b	11	8	18.75	$38 \pm 4$

**Figure 2.** A bismuth target produced by melting bismuth pellets on a hot plate at  $300^\circ\text{C}$  and spreading the bismuth using an ultrasonic soldering iron. The surface is mostly smooth with some ridges and valleys with an average thickness of 66 microns.

by chemical processing results in a more consistent  $^{211}\text{At}$  yield relative to removal of the  $^{211}\text{At}$  by dry distillation. Recent improvements have been made to the ability to reliably produce  $^{211}\text{At}$  at the Cyclotron Institute using the  $(\alpha,2n)$  reaction twelve times over the past 18 months. A summary of the amount of beam available, length of irradiation, and total amount of  $^{211}\text{At}$  produced during each of the runs is shown in Table 1. The amount of  $^{211}\text{At}$  produced is determined by dissolving the target and counting the dissolved solution on an HPGe detector. The asterisk for the amount produced in September 2020 and December 2020 is because the target melted during this irradiation, and the amount of activity had to be estimated by a different means than the other runs. The first two irradiation were done with an alpha beam in the  $+2$  charge state (as denoted by  $^+$  in Table 1. The targets were transferred to Radiochemical Lab 118 within the CI, where the target was dissolved in  $\text{HNO}_3$  and radiochemical experiments were carried out.

Producing a robust bismuth target remains one of the greatest challenges towards astatine production. Bismuth has a relatively low melting point - only  $270^\circ\text{C}$  - resulting

in the potential for melting of the target during irradiation [8]. This melting process alters the geometry of the irradiated bismuth (reducing total astatine production) and can cause the astatine to become volatile. To prevent melting of bismuth targets, we have made significant advancements in the cooling of the bismuth target during irradiation by removing interfaces between the chilled water and the target. The current design uses a single jet, chilled water system flowing directly on the back of the target frame. Additionally, efforts are being made to produce the optimal targets for irradiation and subsequently characterize them for integrity and impurities.

To increase the surface interaction and conductivity between the bismuth and aluminum interface, an ultrasonic soldering iron (S-Bonder SB-9210, S-Bond Technologies, LLC, Hatfield, PA 19440) was used. This method resulted in a stronger adhesion of the bismuth to the aluminum surface and allowed thinner targets, on the order of 50-100 microns, to be produced (shown in Figure 2). Since alpha particles only have enough energy to produce astatine in the first  $70\ \mu\text{m}$  of the bismuth, targets thicker than this are absorbing the alpha energy as heat, further contributing to melting. The thinner targets produced by the ultrasonic soldering iron show promise for maximum  $^{211}\text{At}$  production as well as decreased probability of melting due to the strong bismuth-aluminum interface and  $70\ \mu\text{m}$  target depth.

To investigate the uniformity of the beam at the target position, a Segmented Faraday Cup-Viewer (SFCV) was assembled. The body is made of 3D-printed plastic, with 37 brass screws arranged at regular intervals. Each of these screws acts as a small Faraday Cup, from which beam current can be read via a LabView program, as shown on the left in Figure 3. The body of the viewer was coated with adhesive and CdS, which caused it to fluoresce in the presence of beam, as shown on the right of Figure 3. This gives a much more detailed view of where the beam is situated on the target. A more uniform beam on the target lessens the heat load in any one spot leading to a lower probability of melting the target.

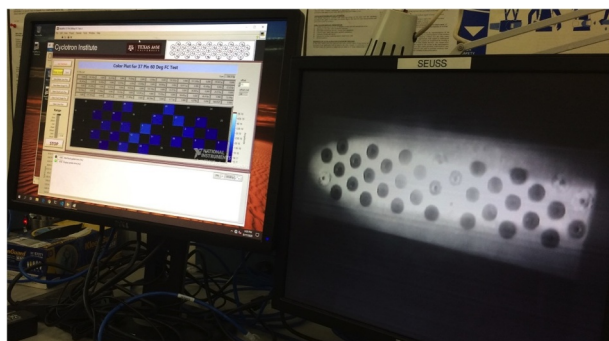


**Figure 3.** Photograph of Segmented Faraday Cup-Viewer (SFCV) being used to tune the alpha beam. The SFCV is 3D printed, with 37 screws which are wired to read the beam current at each disparate position across the target position. The surface has material adhered to it which phosphoresces in the presence of the beam. On the right is a video feed of the SFCV with alpha beam on the target position. On the left is the LabView program reading in the beam current off of each of the disparate screws.

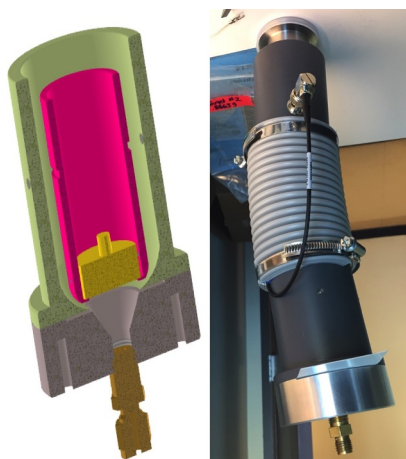


**Figure 4.** Air Monitoring System. Left panel shows a cutaway of the system, where air from the isotope production chamber enters from the top and flows around the pink cylinder, pulled by a pump attached to the gold nozzle. The yellow cylinder indicates the presence of a silicon PIPS detector which detects alpha particles emitted from isotopes caught by the fiberglass filter (not depicted here). Right panel shows a photograph of the actual device. The white card is the fiberglass filter.

Another innovation was electrically isolating the target mounting structure from the rest of the beamline, so that the beam current can be read directly off the target throughout the entire overnight irradiation. This means other Faraday Cups do not need to be dropped in to know how much beam is being delivered to the bismuth target during the irradiation.

Another new aspect of the isotope production process was focused on the safety of those who remove the target from the beamline post-irradiation. Astatine-211 is known to be able to volatilize, particularly if the bismuth target melts during the irradiation. To determine whether this has occurred with any given target, the Air Handling Monitoring System depicted in Figure 4 was developed. The top

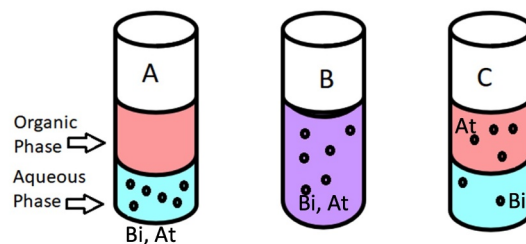


**Figure 5.** Schematic of liquid-liquid extraction process. The organic phase is added to the aqueous phase, containing Bi and At (A). The vial is shaken (B). When the organic and aqueous layers again separate (C), At is in the organic phase, and Bi remains in the aqueous.

of the system attaches to the target chamber. A pump is attached to the bottom of the system. A filter to catch  $^{211}\text{At}$  can be inserted and removed below the silicon detector, as shown. If there is astatine in the air, the silicon detector will measure a characteristic alpha energy, the rate of which will alert the team that it is unsafe to open the chamber at this time. As a double-check, the filter can be removed and counted by a radiation probe, to see whether or not it has alpha contamination.

### 3 At-211 Purification

The near quantitative separation, purification, and recovery of  $^{211}\text{At}$  has been demonstrated at the CI through an extraction chromatography process that uses liquid-liquid extraction as depicted in Figure 5 via porous beads impregnated with 3-octanone, resulting in an elution yield of 92-95% [18]. Moreover, the rapid nature of this process, less than 20 min, was achieved after dissolution of a Bi metal target in  $\text{HNO}_3$  following retrieval from the beamline after  $\alpha$  particle bombardment. The solution was directly loaded onto the column (Figure 6) with no volume or acidity adjustment. The column was washed with  $\text{HNO}_3$  and  $\text{H}_2\text{O}$ , and  $^{211}\text{At}$  was eluted with ethanol, collecting roughly 87 - 93% in 1 mL. This process of recovering high purity  $^{211}\text{At}$ , in near quantitative yields, represents a significant advance in At separations and purification (see Figure 7).

The development of the efficient extraction chromatography process was based on gaining a fundamental understanding of how the At behaves in nitric acid systems. Through a collaboration with Professor M.B. Hall in the Department of Chemistry experimental data was coupled with theoretic computational chemistry to develop new insights into At chemistry. These studies showed that At exists in the trivalent oxidation state as the  $\text{AtO}^+$  species in aqueous nitric acid system. The heavy-element nature of At, and the induced spin-orbit coupling, has a signifi-

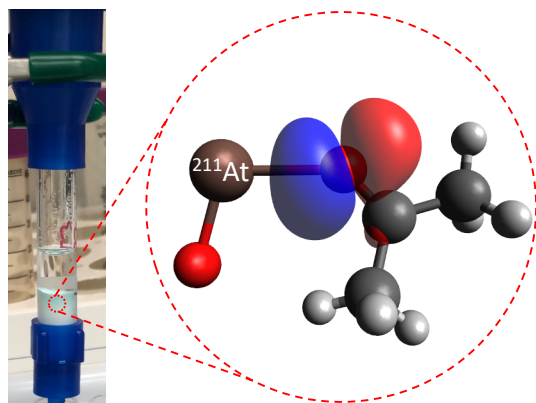


**Figure 6.** Left: Photo of  $^{211}\text{At}$  purification column. Right: Depiction of DFT calculation demonstrating how At-211 interacts with a ketone.

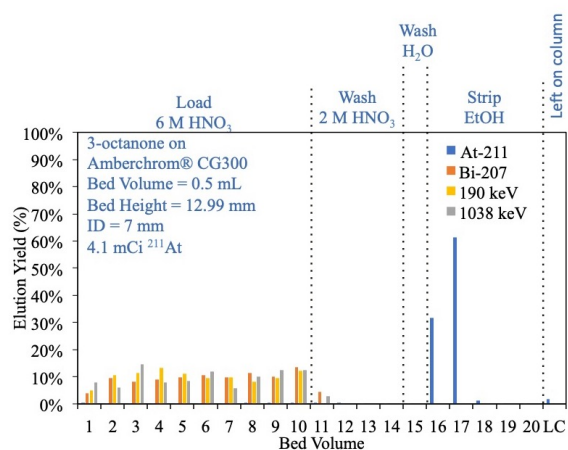


**Figure 7.** Chromatogram of an aliquot of HNO<sub>3</sub> containing the dissolved bombarded target solution with a 3-octanone impregnated Amberchrom®CG300M resin bed.

cant effect on the electronic structure of the  $\text{AtO}^+$  molecular cation, which assumes a pseudo-closed-shell electronic configuration. This closed-shell configuration leads to an enhanced interaction with ketone molecules through a slightly covalent interaction between the  $\text{sp}_2$  hybrid lone pair of the carbonyl oxygen and the lowest unoccupied molecular orbital (LUMO), a non-degenerate  $\pi^*$  orbital, of the  $\text{AtO}^+$ , as shown on the right hand side of Figure 6 [17].

## 4 Characterization

A CdTe detector is utilized to measure the x-rays from the  $^{211}\text{At}$  that has been produced before it is removed from the irradiation chamber. Figure 8 is an example of the spectrum from the Bi target at the end of the irradiation. The 4 peaks at 76.8 keV, 79.2 keV, 89.5 keV, and 92.4 keV are clearly visible indicating the production of astatine.

Two High Purity Germanium (HPGe) detectors are used to measure the hundreds of liquid samples that are

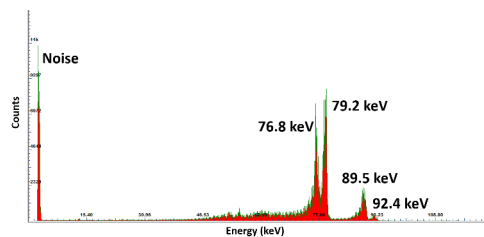


**Figure 8.** CdTe spectrum showing the 4 astatine peaks are 76.8 keV, 79.2 keV, 89.5 keV, and 92.4 keV, respectively.

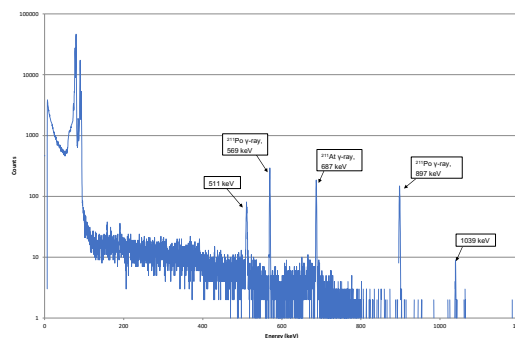


**Figure 9.** Typical HPGe Spectrum showing the characteristic  $\gamma$ -ray of  $^{211}\text{At}$  at 687 keV, as well as peaks belonging to  $^{211}\text{Po}$  and  $^{66}\text{Ga}$ .

produced during the separation chemistry. A spectrum of one of our samples containing  $^{211}\text{At}$  is shown in Figure 9. Below 100 keV, there are many x-rays. The characteristic  $\gamma$ -ray of  $^{211}\text{At}$  is pointed out at 687 keV. The two  $\gamma$ -rays of  $^{211}\text{Po}$  are also labeled at 569 and 897 keV. The other two  $\gamma$ -rays belong to  $^{66}\text{Ga}$  according to our decay curve studies [18], which is separated out by the separation chemistry.

## 5 Summary

Great strides are being made at the CI to improve every aspect of  $^{211}\text{At}$  production. The stability and amount of alpha beam on target, the ability of the targets to handle more beam, and the ability to reliably dissolve the target and separate out the  $^{211}\text{At}$  have all been improved. These advancements are allowing the more reliable production of  $^{211}\text{At}$  for chemistry experiments and may transfer to the ability to produce other alpha emitting isotopes in the future.

## 6 Acknowledgements

The authors are indebted to the operations staff at the Texas A&M University Cyclotron Institute, the Radiological Safety program and M.B. Hall for their contributions to this work. This work was supported by the U.S. Department of Energy Isotope Program, managed by the Office of Science for Isotope R&D and Production under Award No. DE-SC0020958; U.S. Department of Energy under Awards No. DE-NA0003841 and DE-FG02-93ER40773;

Texas A&M University through the Bright Chair in Nuclear Science and the Nuclear Solutions Institute; Texas A&M University System National Laboratories Office and Los Alamos National Laboratory through the joint collaborative research program. LM acknowledges support from the National Science Foundation.

## References

- [1] Makvandi, M.; Dupis, E.; Engle, J. W.; Nortier, F. M.; Fassbender, M. E.; Simon, S.; Birnbaum, E. R.; Atcher, R. W.; John, K. D.; Rixe, O.; Norenberg, J. P. *Target. Oncol.* 2018, 13 (2), 189.
- [2] Li, Y.; Hamlin, D. K.; Chyan, M.-K.; Wong, R.; Dorman, E. F.; Emery, R. C.; Woodle, D. R.; Manger, R. L.; Nartea, M.; Kenoyer, A. L.; Orozco, J. J.; Green, D. J.; Press, O. W.; Storb, R.; Sandmaier, B. M.; Wilbur, D. S. *PLoS One* 2018, 13 (10), e0205135.
- [3] Lambrecht, R. M.; Mirzadeh, S. *Int. J. Appl. Radiat. Isot.* 1985, 36 (6), 443.
- [4] Johnson, E. L. L.; Turkington, T. G. G.; Jaszczak, R. J. J.; Gilland, D. R. R.; Vaidyanathan, G.; Greer, K. L. L.; Coleman, R. E. E.; Zalutsky, M. R. R. *Nucl. Med. Biol.* 1995, 22 (1), 45.
- [5] Dekempeneer, Y.; Keyaerts, M.; Krasniqi, A.; Puttemans, J.; Muyldermans, S.; Lahoutte, T.; Dhuyvetter, M.; Devoogdt, N. *Expert Opin. Biol. Ther.* 2016, 16 (8), 1035.
- [6] Kraeber-Bodere, F.; Rousseau, C.; Bodet-Milin, C.; Mathieu, C.; Guerard, F.; Frampas, E.; Carlier, T.; Chouin, N.; Haddad, F.; Chatal, J.-F.; Faivre-Chauvet, A.; Cherel, M.; Barbet, J. *Int. J. Mol. Sci.* 2015, 16 (2), 3932.
- [7] Elgqvist, J.; Frost, S.; Pouget, J.-P.; Albertsson, P. *Front. Oncol.* 2014, 3, 324.
- [8] Zalutsky, M. R.; Pruszynski, M. *Curr. Radiopharm.* 2011, 4 (3), 177.
- [9] Wilbur, D. S. *Curr. Radiopharm.* 2011, 4 (3), 214.
- [10] Andersson, H.; Cederkrantz, E.; Back, T.; Divgi, C.; Elgqvist, J.; Himmelman, J.; Horvath, G.; Jacobsson, L.; Jensen, H.; Lindegren, S.; Palm, S.; Hultborn, R. J. *Nucl. Med.* 2009, 50 (7), 1153.
- [11] McDevitt, M. R.; Sgouros, G.; Finn, R. D.; Humm, J. L.; Jurcic, J. G.; Larson, S. M.; Scheinberg, D. A. *Eur. J. Nucl. Med. Mol. Imaging* 1998, 25 (9), 1341.
- [12] Kluetz, P. G.; Pierce, W.; Maher, V. E.; Zhang, H.; Tang, S.; Song, P.; Liu, Q.; Haber, M. T.; Leutzing, E. E.; Al-Hakim, A.; Chen, W.; Palmby, T.; Alebachew, E.; Sridhara, R.; Ibrahim, A.; Justice, R.; Pazdur, R. *Clin. Cancer Res.* 2014, 20 (1), 9.
- [13] Zalutsky, M. R.; Reardon, D. A.; Pozzi, O. R.; Vaidyanathan, G.; Bigner, D. D. *Nucl. Med. Biol.* 2007, 34 (7), 779.
- [14] Stickler, J. D.; Hofstetter, K. J. *Phys. Rev. C* 1974, 9 (3), 1064.
- [15] Wilbur, D. *Curr. Radiopharm.* 2008, 1 (3), 144.
- [16] Lucignani, G. *Eur. J. Nucl. Med. Mol. Imaging* 2008, 35 (9), 1729.
- [17] Burns, J. D.; Tereshatov, E. E.; McCarthy, M. A.; McIntosh, L. A.; Tabacaru, G. C.; Yang, X.; Hall, M. B.; Yennello, S. J. *Chem. Commun.* 2020, 56 (63), 9004.
- [18] Burns, J. D.; Tereshatov, E. E.; Avila, G.; Glennon, K. J.; Hannaman, A.; Lofton, K. N.; McCann, L. A.; McCarthy, M. A.; McIntosh, L. A.; Schultz, S. J.; Tabacaru, G. C.; Vonder Haar, A. L.; Yennello, S. J. *Sep. Purif. Technol.* 2021, 256, 117794.